

On the Phase Transitions in Hydrazinium(2+) Sulfate

Takeo OKAMOTO,[†] Nobuo NAKAMURA, and Hideaki CHIHARA*

Department of Chemistry, Faculty of Science, Osaka University, Toyonaka, Osaka 560

(Received January 10, 1979)

The existence of a "diffuse" phase transition below room temperature has been confirmed in $\text{N}_2\text{H}_6\text{SO}_4$ crystal by powder X-ray and DTA experiments. The transition temperature is very sensitive to the grain size. This size effect was discussed on the basis of the thermodynamic nucleation theory taking into account the interfacial energy between the high and the low temperature phases. The diffuse nature of the transition was interpreted by a theory proposed by Tobolsky *et al.* The spin-lattice relaxation times of ^1H were redetermined and the nature of the cationic motion in each phase was discussed.

Hydrazinium(2+) sulfate ($\text{N}_2\text{H}_6\text{SO}_4$) crystallizes in two modifications at room temperature, one orthorhombic and the other monoclinic.¹⁾ The orthorhombic form has been studied extensively by the X-ray and neutron diffraction methods.²⁻⁴⁾ Its crystal structure is described by the space group $\text{D}_2^4\text{-P2}_1\text{2}_1\text{2}_1$ with four formula units in the unit cell; the crystal is ionic and contains distorted $\text{N}_2\text{H}_6^{2+}$ and SO_4^{2-} ions. The N-H bond distances in one of the two NH_3 -groups, $\text{NH}_3(\text{I})$, in an $\text{N}_2\text{H}_6^{2+}$ ion distribute between 0.965 and 0.981 Å and those in the other NH_3 -group ($\text{NH}_3(\text{II})$) between 1.048 and 1.061 Å, the latter seems to form stronger hydrogen bonds with SO_4^{2-} groups than the former. The proton spin-lattice relaxation time T_1 was measured by Harrell and Howell in 1972 and there was found a first order phase transition at 481 K.⁵⁾ More recently Harrell and Peterson measured the spin-lattice relaxation time in the rotating frame, $T_{1\rho}$, in $\text{N}_2\text{H}_6\text{SO}_4$ as well as the line shapes of the deuteron resonance in $\text{N}_2\text{D}_6\text{SO}_4$.⁶⁾ They ascribed each of the two minima observed in both $T_{1\rho}$ and T_1 in the room temperature phase to the reorientation of the NH_3 -groups about the N-N axis and to the 180°-flips of $\text{N}_2\text{H}_6^{2+}$ cation as a whole. They explained the steep decrease in $T_{1\rho}$ above the transition point in terms of translational diffusion of $\text{N}_2\text{H}_6^{2+}$.

Raman spectra were studied with regard to the distortion of the ionic species and the existence of the high temperature phase change at about 200 °C was also reported in Ref. 7. While these NMR and Raman studies failed to "see" any phase transition below room temperature, there is a report on the existence of a phase transition at -50 °C.⁸⁾ This phase transition was recognized by Power *et al.* in the process of their neutron diffraction experiment⁴⁾ and later examined in detail by Caville by Raman measurements.^{9,10)} Caville pointed out that the lowest temperature phase could exist in a metastable state even at room temperature.

We were interested in the nature of the lower phase transition and undertook a differential thermal analysis (DTA) and X-ray measurements on powdered specimens of $\text{N}_2\text{H}_6\text{SO}_4$ as well as remeasurements of proton spin-lattice relaxation time T_1 . This paper reports the results of these experiments; an interesting grain-size dependence of the transition temperature will be described. A possible interpretation for the mechanism of the phase transition will be presented.

[†] Present address: The Institute for Solid State Physics, University of Tokyo, Roppongi, Tokyo 106.

Experimental

Polycrystalline specimens were obtained by recrystallization from an aqueous solution of $\text{N}_2\text{H}_6\text{SO}_4$ (Reagent Grade), followed by desiccation over 4 days. The crystals were ground to fine powders for X-ray, NMR, and DTA measurements. The grain-size effect on the lower phase transition was examined on the specimens which were divided into four parts by use of three sieves of different mesh dimensions. X-Ray powder patterns were obtained with a diffractometer (Rigaku Denki Kogyo Co.) at room temperature ($\approx 18^\circ\text{C}$). Proton magnetic relaxation times were determined by the saturation-90° method with a homemade pulsed spectrometer at 10 MHz. The exponential recovery of the magnetization was confirmed over the entire temperature range of the experiments. The details of the NMR measurements have been published elsewhere.¹¹⁾ DTA experiments were carried out by use of a homemade DTA apparatus with about 1 g of specimen for each experiment. Chromel-*p*-constantan thermocouples (Driver and Harris Co., Ltd.) were used as the thermal sensors. Errors in the temperature measurements were within $\pm 1^\circ\text{C}$.

Results and Discussion

X-Ray Powder Diffraction. Figure 1 shows the X-ray powder patterns obtained at room temperature. Sample I in this figure is a specimen grown from an aqueous solution; the diffraction peaks of this sample were indexed consistently by use of the reported cell dimensions, $a=8.232$, $b=9.145$, and $c=5.535$ Å⁴⁾ together with the intensity data.³⁾ Samples II and III were obtained by cooling Sample I down to 189 and 77 K, respectively, kept at each temperature for a few minutes, and warmed up to the room temperature. One may see that Sample III gives a different powder pattern from that of Sample I, suggesting that the original orthorhombic crystals (hereafter referred to as Phase II) have transformed almost completely into the lowest temperature phase by cooling down to 77 K. Sample II, on the other hand, gives a powder pattern which is a superposition of those of Samples I and III. Therefore, one may understand that the phase transition occurred only in part by cooling down to 189 K. Annealing Sample III at 381 K for 2 h gave the pattern of Sample IV in which the majority of the crystal is transformed back to Phase II but some part still remains as a metastable phase even after the annealing.

Differential Thermal Analysis. A unique behavior of this material as mentioned above was also evidenced by a DTA experiment as shown in Fig. 2. When the

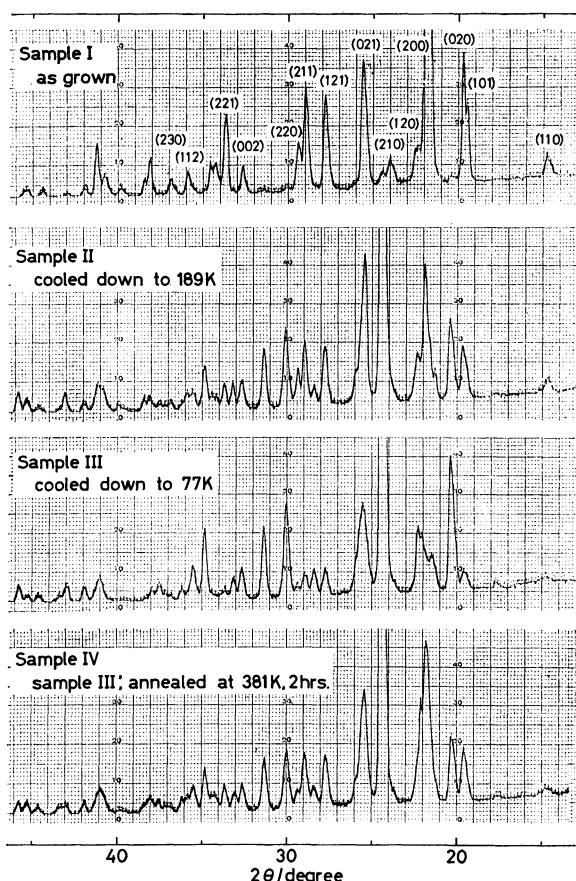


Fig. 1. X-Ray powder diffraction patterns of $\text{N}_2\text{H}_6\text{SO}_4$ at room temperature.

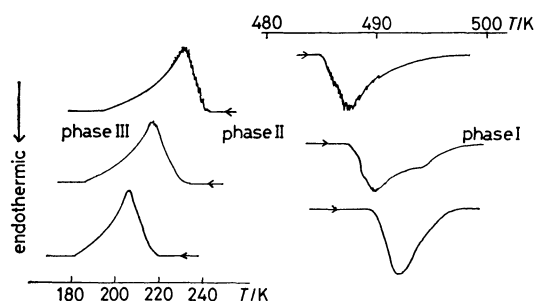


Fig. 2. DTA curves of $\text{N}_2\text{H}_6\text{SO}_4$ obtained by recrystallization (upper curves); after experienced the II→III transition once (middle) and twice (lower).

polycrystalline sample obtained by recrystallization (Phase II) was heated it transformed into Phase I, the highest temperature phase, at 485 K, but the DTA peak associated with this transition had some fine structure. Upon cooling, Phase I transformed into Phase II at 474 K, showing obvious thermal hysteresis as had been observed in Ref. 5. By further cooling a thermal anomaly with fine structure was observed between 242 and 200 K, indicating the transition from Phase II to III. Phase III did not give significant endothermic effect up to 488 K where there is a heat absorption corresponding to the transition from Phase II to I.¹²⁾ This fact suggests that Phase III can exist as a metastable state at least up to room temperature as evidenced in

the X-ray study and can be transformed very gradually to Phase II at higher temperatures in such a way as to show no discernible DTA peaks.

The occurrence of this gradual transition was confirmed by the following experiments: First, after Phase III is heated up to 420 K a small peak was observed on cooling at 234 K, corresponding to the partial transition from Phase II to Phase III. Secondly, when Phase III had been annealed at about 380 K for 12 h it gave an anomaly on cooling at about 230 K as shown in Fig. 2 corresponding to the transition from Phase II to III; thus we concluded that Phase III had been transformed into Phase II during the annealing period.

The feature of the transition from Phase II to III will be summarized as follows: 1) This transition occurs over a very wide temperature range, namely 40 K, 2) the temperature at which the anomaly begins becomes displaced to a successively lower temperature after repeated thermal cycling, and 3) the fine structure in the DTA peak disappears gradually by repeating the thermal cycle. The shift of the transition point as well as disappearance of the fine structure of the DTA peak was also observed at the higher transition from Phase II to I, though only after the material had experienced the lower transition.

Grain-size Effect on the II—III Transition Point.

Among the three characteristics of the II—III transition mentioned above, 2) and 3) may directly be interpreted in terms of a "size effect." The shattering of the crystal upon cooling down through the lower transition has been recognized by Caville.⁹⁾ Let us assume that the specimen with a smaller grain size undergoes the transition from Phase II to III at a lower temperature and that each grain shatters to finer ones as it passes its transition point. It follows then that the apparent transition point should be shifted to a lower temperature after each successive thermal cycle. If there is an

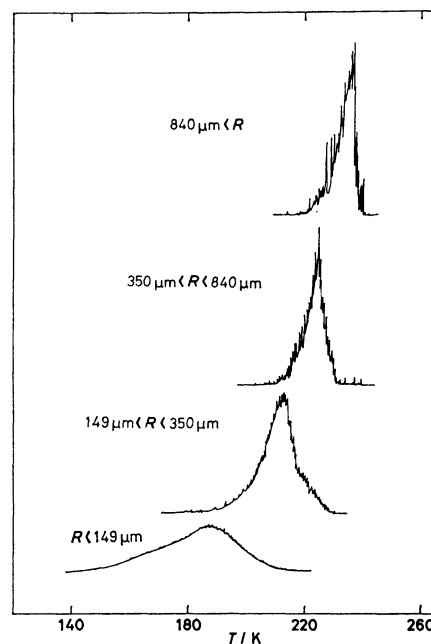


Fig. 3. DTA peaks of II→III transition in specimens with different grain sizes.

ultimate grain size obtained by such thermal cyclings, the specimen would have a homogeneous distribution in grain size and show a single, not composite, DTA peak with no fine structure.

In order to confirm the suggested size effect on the transition point we carried out the DTA on specimens with reasonably defined grain sizes. The results are shown in Fig. 3, which clearly demonstrate that the transition point becomes higher for larger grains. Also the structure of the peak is more prominent for larger grains whereas the transition region spreads broader for smaller grains. By plotting the temperature T_c at which the transition begins to occur against the reciprocal of the average grain size R a linear relation

$$T_0 - T_c = c/R \quad (1)$$

was obtained as given in Fig. 4, with $c=2.36$ mm K and $T_0=237.5$ K (the bulk transition point).

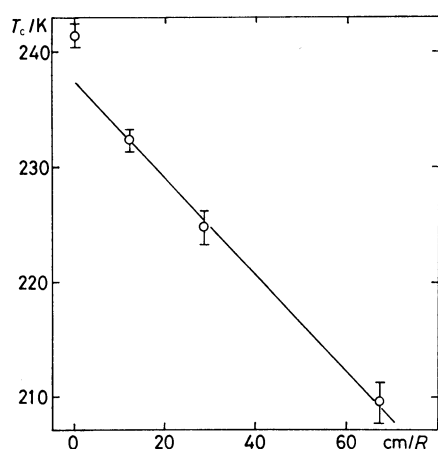


Fig. 4. The II→III transition temperature plotted against the reciprocal of the grain size.

Equation 1 has the form that has been derived for the first order phase transition from thermodynamic considerations which take into account the interfacial energy $\gamma_{\alpha\beta}$ between the high temperature parent modification (α -form) and the low temperature β -form.¹³ There the coefficient depends totally on the "model" of the α - β interface: In the case of the liquid-to-solid phase change c is shown related to γ_{sl} , the interfacial energy between the solid and the liquid through

$$c = 2T_0\gamma_{sl}/L\rho_s \quad (2)$$

by assuming that a spherical nucleus of solid is in equilibrium with the surrounding bulk liquid phase,¹⁴ where L is the latent heat of fusion and ρ_s the density of the solid. On the other hand the relation for the reverse (melting) transition

$$c = (2T_0/L\rho_s)\{\gamma_{sl} + (1 - \rho_s/\rho_l)\gamma_l\} \quad (3)$$

was derived on the assumption that a crystallite can melt below the bulk melting point by the formation of a liquid skin which covers the entire crystal surface so as to make full use of the surface energy of the particle.¹⁵ In this case T_0 is the "skin melting temperature." In Eq. 3 γ_l denotes the surface tension of the liquid and ρ_l the density of the liquid.

Validity of Eqs. 2 and 3 as well as of some other

theoretical models was recently examined in relation to experiments on the melting transition of small lead particles. For the melting of lead particles Eqs. 2 and 3 predicted $c=360$ and 270 nm K, respectively, latter being found close to the experimental results.¹³

The value of c in our present study of II→III solid-solid transition of $N_2H_6SO_4$ is surprisingly large in comparison with that for the melting transition of lead (by a factor of 10^4). Although a value of c can not be estimated theoretically for $N_2H_6SO_4$ because of the lack of the knowledge of the interfacial energies, it seems that not only the interfacial energy but also some other factors will contribute to the large supercooling phenomenon. These factors are, e.g., the large molecular misfit across the boundary of the two phases,¹⁶ and the facility with which the nucleus of the new phase is formed in the mother crystal.¹⁷

In the case of the phase transition from Phase II to I the DTA peak is displaced to the higher temperature side as the grains become finer. This tendency is opposite to that in the II→III transition. If one is to apply Eq. 3 for the II→I transition, the surface tension of Phase I, γ_I , must be larger than $\gamma_{I,II}/(\rho_{II}/\rho_I - 1)$. Since ρ_{II} could be larger than ρ_I no more than 10%, this would mean that $\gamma_I > 10\gamma_{I,II}$ which is very questionable. Therefore, there will be other reason or reasons for the shift of the transition point in the II→I transition.

Diffuseness of the II—III Transition. As is pointed out in a previous section the phase transition between Phases II and III occurs gradually over a wide range. The possible origin of such a sluggish or diffuse phase transition was examined by Tobolsky *et al.*¹⁸ They developed an *a posteriori* theory for the diffuse phase transition which is by nature the transition of the first order but actually occurs over a wide temperature range. They postulated the existence of a boundary phase K between two different phases A and B which are stable at high and low temperatures, respectively.

By solving for eigenvalues of an Ising matrix of molecular partition functions f_A, f_B , and f_K they obtained an expression for the number n_A or the number fraction x_A of molecules in the phase A as

$$x_A = \frac{n_A}{n_0} = \frac{1 - y + (\epsilon y)^{1/2} + [(1 - y)^2 + 4(\epsilon y)^{1/2}]^{1/2}}{(1 - y)^2 + 4(\epsilon y)^{1/2} + (1 + y)[(1 - y)^2 + 4(\epsilon y)^{1/2}]^{1/2}} \quad (4)$$

where

$$y = \exp(-\Delta G_t/RT) \quad (5)$$

and

$$\epsilon = \exp(-2\Delta G_K/RT). \quad (6)$$

Here ΔG_t and ΔG_K are changes of the molar Gibbs functions associated with A-to-B and A-to-K transitions, respectively, the latter being taken as infinite for an infinitely sharp transition. The expressions of x_B and x_K has also been given in Ref. 18. The anomalous part $\Delta C_p(T)$ of the heat capacity at a temperature T is written as

$$\Delta C_p(T) = -\{(\Delta H_t)^2/RT^2\}y(dx_A/dy) \quad (7)$$

where ΔH_t is the molar enthalpy change in the transition.

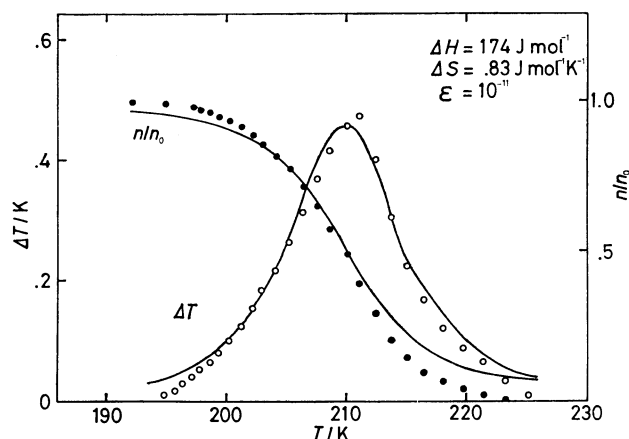


Fig. 5. The DTA curve (open circles) and the fraction of molecules in Phase III (filled circles) in II→III transition of the specimen with $149 \mu\text{m} < R < 350 \mu\text{m}$.

Tobolsky *et al.* applied the theory to the heat capacity anomaly in several materials in detail and found that the heat capacity curve can be described using only one numerical parameter, ϵ or ΔG_k . In the present case of $\text{N}_2\text{H}_6\text{SO}_4$ no heat capacity data are available. But the shape of the anomaly in the DTA curve reasonably represents what one would expect for the anomalous part of the heat capacity curve. Thus, as an example, the DTA curve in the cooling direction for the specimen of the size $149 \mu\text{m} < R < 350 \mu\text{m}$ in Fig. 3 was then fitted to Eqs. 4 and 7, the result being shown in Fig. 5. In this figure the fraction of the low temperature phase n/n_0 at each temperature was obtained by integrating the DTA thermogram (the height of which stands for ΔT , the temperature difference between the reference material and the sample under investigation).

Such a fitting gave the thermodynamic functions for the transition the values, $\Delta H_t = 174 \text{ J mol}^{-1}$, $\Delta S_t = 0.83 \text{ J mol}^{-1} \text{ K}^{-1}$, and $\epsilon = 10^{-11}$, corresponding to $2\Delta G_k \approx 44 \text{ kJ mol}^{-1}$. ΔG_k , the Gibbs energy of formation of a boundary phase K from Phase II, is not too large to neglect the formation of the phase K in the transition from Phase II to III. The disappearance of the reverse phase transition in the heating run as mentioned in the preceding section can also be accounted for if $\epsilon > 10^{-7}$ is assumed for the formation of phase K from Phase III. In such a case the theoretical curve becomes so flat that one can hardly "observe" any evidence of the phase transition.

The postulate of the boundary phase K has no direct bearing with the particle size effect but it certainly will be one form of manifestation of the significance of the interface energy. Unfortunately it is not possible to relate the value of ΔG_k derived here to any realistic structural model of the transition.

Spin-lattice Relaxation Time. Since the general nature of the phase transitions in $\text{N}_2\text{H}_6\text{SO}_4$ has been understood in the X-ray and the DTA experiments, we proceed to the results of measurements of the spin-lattice relaxation time T_1 on a polycrystalline sample in order to shed some light on the type of motion that $\text{N}_2\text{H}_6^{2+}$ cations undergo in each phase.

The results are shown in Fig. 6. On heating the

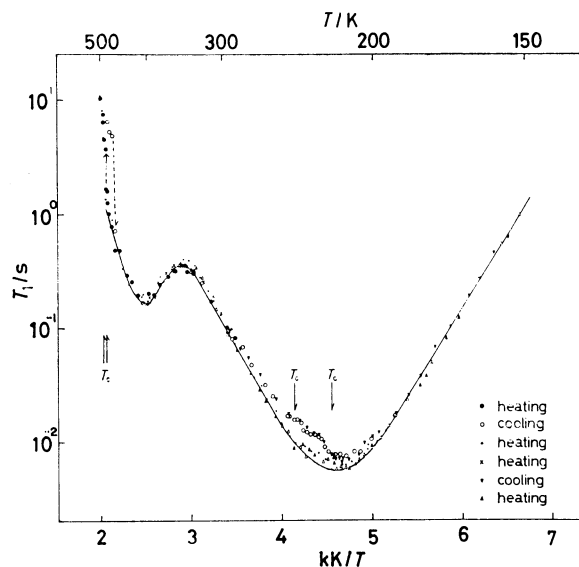


Fig. 6. T_1 of ^1H in polycrystalline $\text{N}_2\text{H}_6\text{SO}_4$ at 10 MHz. The two pairs of arrows indicate the transition regions. The solid curve is calculated with Eqs. 8 and 9. For the illustration of the symbols see in text.

specimen obtained by recrystallization from room temperature upwards the T_1 behavior was very similar to that reported by Harrell and Howell⁵⁾ as shown by filled circles in Fig. 6. However, on initial cooling of Phase II, the values of T_1 longer than those given in Ref. 5 were obtained (open circles); we also observed a significantly irregular behavior of T_1 in the transition region between about 210 and 250 K as will be described in the following. On heating, Phase III gave T_1 value shorter than those in Phase II, the former being shown by dots and open triangles.

Our values of T_1 for Phase III agree with the Harrell and Howell's results, indicating that what they were looking at was Phase III without being aware of the occurrence of the II—III transition when they cooled their specimen. As one sees in Fig. 6 the difference in T_1 between Phases II and III becomes smaller with increase in temperature and converges to zero somewhere around 300 K. This fact suggests that the transition from Phase III to II proceeds continuously during the T_1 measurements.

The T_1 data were interpreted according to the BPP type of formulation for the dipole-dipole interaction between protons in the form¹⁹⁾

$$T_1^{-1} = K \{ \tau_c / (1 + \omega_0^2 \tau_c^2) + 4\tau_c / (1 + 4\omega_0^2 \tau_c^2) \} \quad (8)$$

where ω_0 is the Larmor frequency of the nuclear spin, τ_c the correlation time of a specified motion, and K a factor representing reduction of the strength of dipolar interaction due to that motion. If the two crystallographically nonequivalent NH_3 -groups rotate about their figure axes (C_3 -rotation) with different correlation times (τ_{ci}), the relaxation rate can be written as

$$T_1^{-1} = 1/2 \sum_i K_i \{ \tau_{ci} / (1 + \omega_0^2 \tau_{ci}^2) + 4\tau_{ci} / (1 + 4\omega_0^2 \tau_{ci}^2) \}, \quad i = 1, 2. \quad (9)$$

By fitting Eq. 9 to the experimental T_1^{-1} curve in Phase III as shown in Fig. 6 by solid line the activation

TABLE 1. THE ACTIVATION PARAMETERS FOR THE MOTION OF $N_2H_6^{2+}$ CATIONS

Phase	Mode of Motion	$K/10^8$ s^{-1}	E_a/kJ mol^{-1}	$\tau_0/10^{-15}$ s
I	Translational diffusion ^{a)}	—	184	—
II	C_3 -rotation of NH_3 -group	—	24.9	—
	180° -flip of $N_2H_6^{2+}$	2.5	54.0	1.0
	180° -flip of $N_2H_6^{2+a)}$	1.9	40.5	166
III	C_3 -rotation of $NH_3(I)$	104	24.9	7.9
	C_3 -rotation of $NH_3(II)$	66	27.8	3.9
	C_3 -rotation of $NH_3^b)$	—	26.2	6.0

a) Ref. 6. b) Ref. 6. A single correlation time was assumed for the motion of two kinds of NH_3 -groups.

energies and τ_{0i} 's were obtained for the C_3 -rotation as listed in Table 1. Here the Arrhenius activation process was assumed for the motion:

$$\tau_{ci} = \tau_{0i} \exp(E_{ai}/RT). \quad (10)$$

Of the two sets of values for activation parameters for Phase III, the one with the smaller E_a and the larger K may be assigned to $NH_3(I)$ and the other set to $NH_3(II)$. This is because $NH_3(II)$ forms stronger hydrogen bonding with the surrounding SO_4^{2-} groups than $NH_3(I)$ does.

Only the average activation energy was calculated for the C_3 -rotation in Phase II from the slope of $\ln T_1$ vs. $1/T$ between 250 and 295 K by assuming $\omega_0\tau_c \ll 1$ (see in Table 1). The activation parameters for the 180° -flip of $N_2H_6^{2+}$ were obtained by fitting Eq. 8 to the observed T_1^{-1} by assuming that the correlation time of this motion is so large in comparison with τ_c of C_3 -rotation that the two modes of motion can be treated independently. The analysis gave E_a and τ_0 in Table 1 and the solid line in Fig. 6.

The activation energy and τ_0 for the 180° -flip of $N_2H_6^{2+}$ in the present work are significantly different from those in Ref. 6 which have been deduced from the T_1 data. Such a discrepancy may have come from the ambiguity in fitting the theoretical T_1 curve to the experimental one in a rather narrow temperature range.

It is interesting to note, however, that the free energy of formation of a boundary phase K between Phases II and III is comparable to the activation energy for the 180° -flip of $N_2H_6^{2+}$, suggesting some rearrangement of

$N_2H_6^{2+}$ cations takes place in the phase change process.

We are grateful to Mr. Takechika Iida for his assistance in the DTA measurements. Acknowledgment is made to the Mitsubishi Foundation for financial support of this research.

References

- 1) P. Groth, "Chemische Krystallographie," Verlag von Wilhelm Engelmann, Leipzig (1908), II. Teil, p. 385.
- 2) I. Nitta, K. Sakurai, and Y. Tomiie, *Acta Crystallogr.*, **4**, 289 (1951).
- 3) P. G. Jonsson and W. C. Hamilton, *Acta Crystallogr., Sect. B*, **26**, 536 (1970).
- 4) L. F. Power, K. E. Turner, and J. A. King, *Acta Crystallogr., Sect. B*, **31**, 2470 (1975).
- 5) J. W. Harrell, Jr. and F. L. Howell, *J. Magn. Reson.*, **8**, 311 (1972).
- 6) J. W. Harrell, Jr. and E. M. Peterson, *J. Chem. Phys.*, **63**, 3609 (1975).
- 7) M. Guay, J. Weber, and R. Savoie, *Can. J. Spectrosc.*, **19**, 127 (1974).
- 8) P. Pepinsky, K. Vedam, Y. Okaya, and S. Hoshino, *Phys. Rev.*, **111**, 1467 (1958).
- 9) C. Caville, *Can. J. Spectrosc.*, **20**, 123 (1975).
- 10) C. Caville, *Solid State Commun.*, **21**, 475 (1977).
- 11) T. Tsuneyoshi, N. Nakamura, and H. Chihara, *J. Magn. Reson.*, **27**, 191 (1977).
- 12) In our course of the DTA experiments a small and very broad endothermic anomaly has occasionally been observed above 330 K, indicating the probable occurrence of the transition from Phase III to Phase II, but we could not ascertain the necessary conditions for the reproducibility of such an anomaly.
- 13) S. J. Peppiatt and J. R. Sambles, *Proc. R. Soc. London, Ser. A*, **345**, 387 (1975) and the references therein.
- 14) E. Rie, *Z. Phys. Chem.*, **104**, 354 (1923).
- 15) A. E. Curzon, Thesis, 1960, University of London, cited in Ref. 13.
- 16) D. Turnbull, "Solid State Physics," ed by F. Seitz and D. Turnbull, Academic Press, New York (1956), Vol. 3, p. 225.
- 17) M. J. Buerger, "Phase Transformations in Solids," ed by R. Smoluchowski, J. E. Mayer, and W. A. Weyl, John Wiley and Sons, New York (1951), p. 183.
- 18) A. V. Tobolsky, J. J. Kozak, and N. H. Canter, *Phys. Rev.*, **138**, A651 (1965).
- 19) A. Abragam, "The Principles of Nuclear Magnetism," Oxford, London (1961), Chap. 8.